Journal of Innovative Image Processing (ISSN: 2582-4252)
www.irojournals.com/iroiip/

Advancing PCOS Diagnosis: Capsule Network-Based Classification using Ultrasound Images

Venkatesh G.[1], Bajulunisha A.[2], Sreenivasa Rao Chappidi[3], Karthikeyan S.[4], Dhivya K.[5], Murugan S.[6]

[1]Department of Computer Science and Engineering, Koneru Lakshmaiah Education Foundation, Andhra Pradesh, India

[2]Department of Computer Science and Engineering, Chennai Institute of Technology, Chennai, India.

[3] Department of Electronics and Communication Engineering, Vardhaman College of Engineering, Hyderabad, India

[4]Department of Electronics and Communication Engineering, K.S.R. College of Engineering, Tiruchengode, India

[5]Department of Electronics and Communication Engineering, SRM Institute of Science and Technology, Kattankulathur, Chennai, India

[6]Department of Biomedical Engineering, Saveetha School of Engineering, Chennai, India

E-mail: [1]gandavadi.venkatesh@gmail.com, [2]nbajulu.cse2011@gmail.com, [3]sreenivasa1715@vardhaman.org, [4]skkn03@gmail.com, [5]dhivyakesavan2006@gmail.com, [6]smuresjur@gmail.com

Abstract

Capsule Networks have been developed as an alternative to Convolutional Neural Networks (CNN) for encapsulating spatial hierarchies in images or signals. The objective is to improve the precision of Polycystic Ovary Syndrome (PCOS) classification by sophisticated image processing methodologies. The proposed system uses the features of Capsule Networks to examine medical ultrasound images for PCOS classification while improving feature protection. It creates a reliable diagnostic model capable of accurately differentiating between healthy and PCOS. Capsule Networks provide more detailed evaluations of ovarian morphology by preserving the orientation and positioning information of characteristics. Three different capsule networks, such as Dynamic Routing CapsNet (DRCN), Expectation-Maximization (EM) Routing CapsNet (EMRCN), and Deep CapsNet (DCN), are analyzed for PCOS classification using more than 3000 images in the PCOS dataset. Results prove that the

DOI: https://doi.org/10.36548/jiip.2025.1.011
Received:02.03.2025, received in revised form: 28.03.2025, accepted:13.04.2025, published: 25.04.2025

proposed Deep Capsule Network achieves better overall accuracy of 99.33 %, sensitivity of 99.27 %, and specificity of 99.4 % compared to other types of capsule networks. The combination of Capsule Networks with medical imaging procedures presents a promising framework for timely and precise diagnosis, thereby diminishing diagnostic delays and enhancing patient outcomes in gynaecological healthcare systems.

Keywords: Capsule Networks, Polycystic Ovary Syndrome, Medical Image Processing, Ultrasound Diagnosis, Deep Learning Models.

1. Introduction

A large percentage of reproductive-age women have Polycystic Ovary Syndrome. PCOS may cause infertility, diabetes, and cardiovascular disease, thus, early identification is essential for treatment. Traditional diagnostic methods include clinical evaluations, hormonal measurements, and ultrasound imaging. These images vary in appearance, operator dependency, and subjective judgment, making manual interpretation difficult. Automated and trustworthy medical image diagnostic approaches using sophisticated machine learning models are needed for early diagnosis [1-2]. Capsule Networks, a unique deep learning architecture that overcomes the constraints of Convolutional Neural Networks, are used to improve PCOS diagnosis accuracy. Capsule Networks can capture hierarchical connections and spatial patterns in images, making them ideal for medical imaging jobs that require detecting tiny, local components like ovarian follicles. These unique qualities are used to construct an automated system that outperforms conventional approaches in dependability and accuracy.

Multiple symptoms and minor morphological markers in medical imaging make PCOS a complicated endocrine disorder that affects reproductive-aged people difficult to identify. Convolutional Neural Networks (CNNs) fail to grasp ultrasound images' complicated spatial hierarchies, resulting in inaccurate diagnosis. Capsule Networks preserve spatial correlations between image characteristics and provide a potential solution with dynamic routing and vector-based design. An accurate, trustworthy, and interpretable AI model that analyses high-dimensional ultrasound images while keeping the ovarian pattern structure is needed. Optimising model input requires contrast improvement, noise reduction, and segmentation. Deep learning algorithms customised for medical image interpretation will be used to construct a robust disease detection model that outperforms current models to reduce diagnostic delays and variability [3-4].

1. **Preservation of Spatial Hierarchies:** Ultrasound images of ovaries often contain subtle differences in follicle arrangement and structure. Unlike CNNs, DCNs retain spatial relationships between image features, which is essential for distinguishing between normal and polycystic ovarian patterns.
2. **Better Handling of Rotation and Pose Variations:** In ultrasound imaging, the angle and orientation of the ovary can vary. DCNs use dynamic routing between capsules to maintain robustness to pose and viewpoint changes, making them ideal for such clinical imaging tasks.
3. **Reduced Dependence on Data Augmentation:** Since DCNs are inherently more invariant to affine transformations, they require less data augmentation to generalize well, which is beneficial in medical domains where annotated data is limited.
4. **Efficient Feature Encoding:** Capsules represent not just the presence of a feature, but also its instantiation parameters (e.g., orientation, scale), which enhances the model's ability to differentiate between closely resembling ovarian tissues.
5. **Improved Classification Confidence:** DCNs provide vector outputs whose length indicates the probability of class presence, making them more interpretable and reliable in clinical diagnosis compared to scalar outputs from CNNs.

The research is structured as follows: PCOS diagnosis using machine learning and deep learning is addressed in Section 2. It argues for Capsule Networks by highlighting the drawbacks of CNN-based approaches. Capsule Networks handle spatial information and object relations well in medical imaging. Section 3 discusses the proposed methodology's technical specifics. Capsule Networks are presented as a basic component, focusing on their design and how dynamic routing techniques increase detection accuracy. How advanced image processing improves ultrasound images for analysis is also explained. A complete PCOS diagnosis system combines Capsule Networks with various methods. Section 4 discusses experimental setup, dataset features, and system performance measures. Comparisons with typical CNN models concentrate on diagnostic accuracy, sensitivity, specificity, and computational economy. The part also tests Capsule Networks under different imaging settings and dataset sizes to assess their resilience. Section 5 summarizes the results, emphasizing Capsule Networks and sophisticated image processing methods that improve PCOS identification. Hybrid models and bigger annotated datasets may increase detection accuracy, but computational loads and dataset availability limit detection accuracy.

2. Literature Survey

Machine learning approaches for PCOS detection have gained attention for their potential to automate diagnostic processes. In [5], a machine learning-based framework was introduced for PCOS detection using Capsule Networks, focusing on pattern recognition within ovarian images. This method provides an efficient way to identify and monitor PCOS symptoms. The regulation and polarization of macrophages within ovarian tissues of PCOS patients were explored in [6]. This analysis examined the behaviour of macrophages in the ovarian microenvironment, emphasizing the importance of the immune response in PCOS pathology. A comprehensive review and meta-analysis of randomized controlled trials investigating the use of Kuntai capsules for treating ovulatory disorder infertility were performed in [7]. This meta-analysis evaluated the efficacy of Kuntai capsules, a traditional Chinese medicine, in restoring ovulation and improving fertility outcomes. In [8], the therapeutic effects of mesenchymal stem cell-derived apoptotic vesicles on ovarian folliculogenesis were evaluated. These vesicles demonstrated an ability to reverse impaired ovarian functions in PCOS and ovarian aging by modulating the WNT signalling pathway.

An integrative approach combining network pharmacology and experimental verification was applied to explore the mechanism of YJKL Decoction for treating PCOS-related infertility in [9]. This research utilized bioinformatics tools to map the molecular pathways influenced by the herbal decoction, uncovering key regulatory processes. The antioxidant properties of Sinapic acid and its effects on oxidative stress and metabolic disturbances in a rat model of PCOS were investigated in [10]. Sinapic acid demonstrated the ability to reduce ovarian fibrosis and mitigate PCOS symptoms by restoring metabolic balance. A comprehensive review of the pathogenesis and essential factors contributing to PCOS was conducted in [11]. This work examined the underlying hormonal, metabolic, and environmental triggers that exacerbate PCOS symptoms, enabling a detailed understanding of how these factors interplay in the onset and progression of the condition. By exploring these mechanisms, the research provided a foundation for developing targeted interventions to address the root causes of PCOS. In [12], the effect of Oligopin administration on ovarian morphology in women with PCOS was examined. Oligopin, a pine extract, was shown to have a significant impact on reducing ovarian cysts and improving hormonal imbalances in patients.

New perspectives on diagnosing and treating PCOS were presented in [13], which reviewed modern methods, including advancements in diagnostic imaging and hormonal therapies. The research addressed how evolving medical technologies have refined the diagnostic criteria for PCOS, allowing for more accurate detection. The molecular mechanisms behind the effects of Bushen Tiaoxue Granules on ovarian hyperstimulation-induced endometrial abnormalities were analysed using network pharmacology in [14]. The granules showed protective effects on the endometrium by modulating hormone levels and oxidative stress markers. A study on the reprogramming of human fibroblasts into ovarian granulosa-like cells through FOXL2 and NR5A1 expressions was conducted in [15]. This innovative approach demonstrated how fibroblasts can be transformed into functional ovarian cells, enabling a potential breakthrough in fertility treatments.

The ongoing public health concerns surrounding PCOS were explored in [16]. This emphasized the increasing prevalence of PCOS and its long-term health implications, including diabetes, cardiovascular diseases, and reproductive issues. In [17], the impact of consultation frequency on the assessment and treatment of PCOS was analysed. The study found that repeated consultations led to improved treatment outcomes by allowing for more accurate assessments of hormonal levels and ovarian morphology. A cutting-edge method for diagnosing cardiac diseases using the Mamba Capsule Network was introduced in [18]. The technique demonstrated the network’s utility in processing electrocardiographic data, showing high accuracy in detecting arrhythmias. While focused on cardiac diseases, the Capsule Network’s potential for processing complex medical data suggested its applicability in other areas, such as PCOS detection through ultrasound imaging. Capsule Networks with dynamic routing were utilized for classifying benign and malignant lung cancer using computed tomography images in [19]. The dynamic routing capabilities of Capsule Networks allowed for better handling of spatial hierarchies in medical images, making them suitable for complex classifications.

The development of deep multi-prototype Capsule Networks was discussed in [20], where each class of input data was represented by multiple prototypes. This improved the ability of Capsule Networks to classify heterogeneous data, reducing misclassification rates. A Two-Stream spectral-spatial Capsule Network for hyperspectral image classification was proposed in [21]. This method integrated spectral and spatial information to enhance classification performance, particularly in high-dimensional datasets. In [22], a 3D Capsule Network designed for video-based facial expression recognition was introduced. This network focused on capturing temporal changes in expressions over time. A Capsule Network model incorporating contrastive learning for depression detection was presented in [23]. By comparing positive and negative samples, the model was able to identify subtle patterns linked to depressive symptoms. The role of Capsule Network projectors as equivariant and invariant learners was explored in [24]. This research demonstrated how Capsule Networks could maintain consistency in classifying data even when subjected to transformations such as rotation or scaling.

3. Proposed System

The proposed approach uses Capsule Networks to improve PCOS detection using image processing methods. Traditional convolutional neural networks lose spatial hierarchies during pooling, rendering them unsuitable for ovarian ultrasound analysis. Capsule Networks preserve part-to-whole links, which are necessary to recognise PCOS structural patterns. Three different types of architecture, like DRCN, EMRCN, and DCN are used in this approach.

- **DRCN** lets capsules selectively activate important characteristics, improving model interpretability and accuracy.
- **EMRCN** models posture parameters and presence probability to improve feature representation.
- **DCN** allows more complicated hierarchies and multi-level abstractions to capture small follicular arrangement changes. Advanced preprocessing methods include segmentation, contrast enhancement, and noise filtering optimise feature extraction.

3.1 Dynamic Routing CapsNet

CapsNets was a breakthrough in deep learning [25]. Traditional Convolutional Neural Networks (CNNs) use pooling operations that lose spatial information, making it difficult to recognise feature correlations. CapsNets retain spatial hierarchies and part-whole linkages utilising dynamic capsule routing, providing a more organised knowledge of images and objects. Multiple layers of DRCN capture local and global feature dependencies. Starting with a 9x9 convolution layer, it collects low-level information from the input image. This repeated approach improves generalisation and reduces mistakes in complicated visual tasks by passing on only relevant information. Figure 1 shows the DRCN architecture from input to classification.

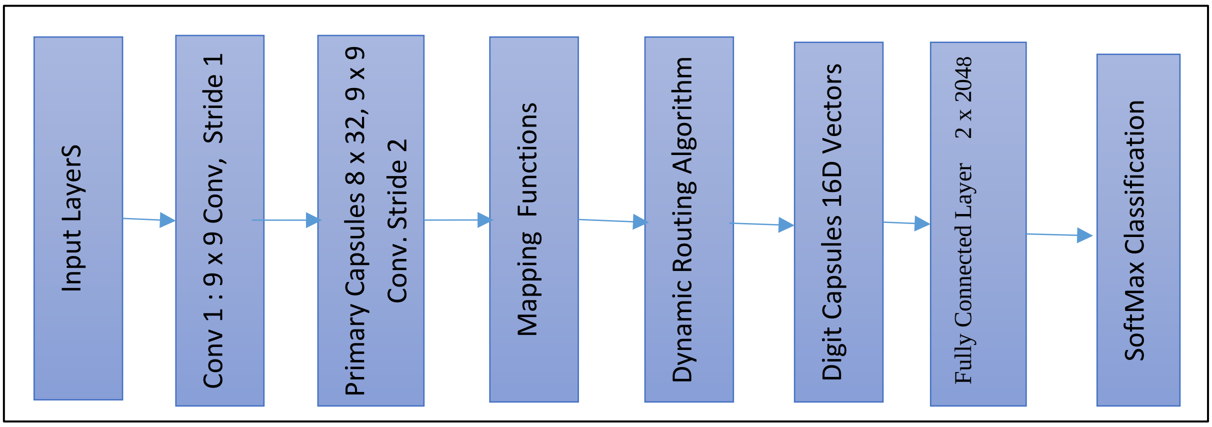

Figure 1. Architecture

Initial design includes a 9x9 convolutional layer for extracting low-level characteristics from the input image. In the Primary Capsules layer, 9x9 convolutions with stride 2 capture spatial correlations. Equation Representation of dynamic routing is shown in Equation 1.

$$v_j = \text{squash}\left(\frac{\exp(b_{ij})}{\sum_k \exp(b_{ik})}\right) . W_{ij} u_i \tag{1}$$

Mapping shown in Equation 2 follows the main capsule generation. This function is essential for capsule networks because it keeps each capsule's output vector length between 0 and 1, signifying the input's probability of a certain entity. The formula is.

$$v_j = \frac{s_j^2}{1+ s_j^2} \cdot \frac{s_j}{s_j} \tag{2}$$

where s_j is the input to capsule j and v_j is the mapped output. This vector-specific mapping retains the capsule's output direction while normalising its length, unlike ReLU or sigmoid. After mapping, the dynamic routing Algorithm appears twice in the design, representing two routing steps or the iterative process. This method dynamically changes information flow between subsequent capsule layers. Based on how closely the expected output of a lower-level capsule matches the actual output of a higher-level capsule, it repeatedly updates coupling coefficients. Capsules "vote" on which higher-level capsules get their information, helping the network understand part-whole linkages. The Digit Capsules layer, which represents output classes like 0–9, follows. A 16-dimensional vector representing existence, orientation, scale, and other pose-related properties is produced by each digit capsule. The length of this vector indicates the probability of that digit in the input. The Pseudocode (Pseudocode 1) for DRCN is as follows:

Input:

u_i → Output vectors from lower-level capsules

W_ij → Transformation matrices (learnable)

r → Number of routing iterations

Output:

v_j → Output vectors from higher-level (digit) capsules

1. for all capsules i in lower layer and capsules j in higher layer:

compute predictions: û_ij = W_ij * u_i

2. initialize routing logits: b_ij = 0 for all i, j

3. for routing iteration t = 1 to r do:

for all capsules i:

$\boldsymbol{c_{ij}} = \frac{\exp(b_{ij})}{\sum_{\boldsymbol{k}} \exp(b_{ij})}$ // normalize routing weights over j

for all capsules j:

$s_j = \sum_i c_{ij} \,.\, u_{ji}$ // weighted sum of predictions

$v_{ji} = \frac{\|s_j^2\|}{1+ s_j^2} \cdot \frac{s_j}{\|s_j\|}$ // non-linear mapping function

for all capsules i, j:

$b_{ij} \leftarrow b_{ij} + u_{ji} \,.\, v_j$ // **dot product (agreement)**

return v_j

Pseudocode 1. Pseudocode of DRCN

3.2 EM Routing CapsNet

EMRCN as an extension of DRCN [26]. The original CapsNets kept spatial hierarchies, but the routing algorithm struggled to allocate capsule activations, especially in deep structures. EMRCN optimises lower-level capsule information routing to higher-level capsules using an EM method. The approach weights capsules correctly, minimising redundancy and boosting classification accuracy, particularly in deeper networks. EMRCN architecture, shown in Figure 2, enhances capsule networks utilising the routing algorithm. A mapping function follows capsule formation. Special non-linear activation for capsule networks. It turns each capsule's output vector into a probability-like representation by ensuring its length is between 0 and 1. Vector direction conveys instantiation parameters (e.g., posture, scale), whereas magnitude reflects feature present probability. EMRCN, an advanced dynamic routing algorithm, processes capsule outputs. EM routing iteratively refines capsule coupling across layers using Expectation-Maximization, unlike vector similarity approaches. In each cycle, lower-level capsules distribute their outputs to higher-level capsules depending on how well they fit a Gaussian distribution modelled by them. This helps the network represent complicated hierarchies. Routers create digit capsules layers. Digit capsules provide 32-dimensional vectors that include precise information about a class, such as digits 0–9 for digit recognition. This vector's length influences class probability, whereas its direction encodes pose-specific class information.

EM Routing is a probabilistic routing mechanism between capsules. It estimates how likely each lower capsule belongs to a higher-level capsule using Expectation-Maximization explained in Equation 3. Compute assignment probabilities r_{ij} using.

$$r_{ij} = \frac{p\left(c_j\right) . \mathcal{N}\left(u_i \mid \mu_j, \sigma_j^2\right)}{\sum_k p\left(c_k\right) . \mathcal{N}\left(u_i \mid \mu_k, \sigma_j^2\right)} \qquad (3)$$

where u_i is vote from capsule i, μ_j, σ_j is mean and variance of the Gaussian modeled by capsule j , $p\left(c_j\right)$ is activation probability of capsule j , $\mathcal{N}$ is Gaussian likelihood.

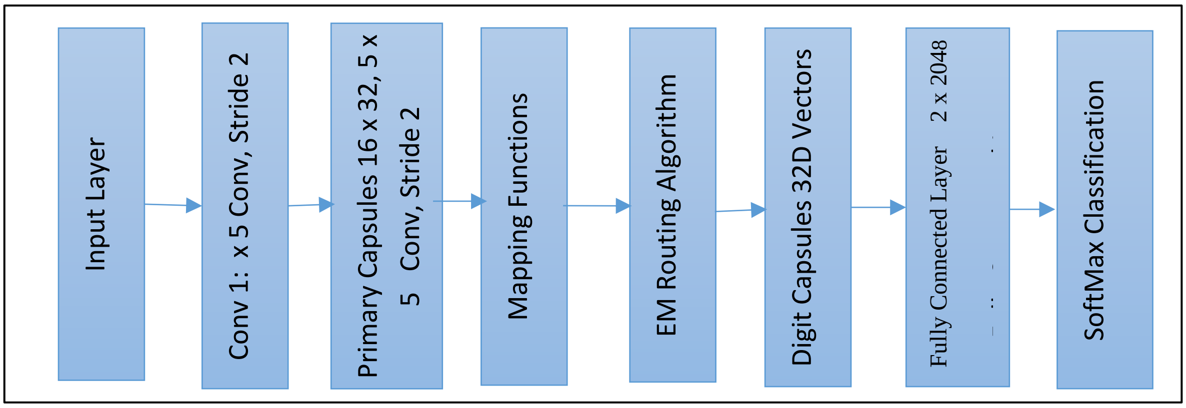

Figure 2. EMRCN Architecture

The Pseudocode (Pseudocode 2) of EMRCN is as follows.

Input:

```
    u_i      → Pose matrices from lower-level capsules
    a_i      → Activation probabilities of lower-level capsules
    W_ij     → Transformation matrices
    r        → Number of EM routing iterations
Output:
    v_j      → Pose matrices of higher-level capsules
    a_j      → Activation probabilities of higher-level capsules
1. for all capsules i and j:
      compute votes: û_ij = W_ij * u_i
2. initialize routing assignment probabilities:
      r_ij = 1 / number of higher-level capsules
3. for iteration t = 1 to r do:
      // M-step: update Gaussian parameters for each capsule j
      for all capsules j:
         r̂_ij = a_i * r_ij    // weighted responsibilities
         sum_r̂ = ∑_i r̂_ij
```

$\mu_j = \frac{\sum_i a_i \, r_{ij} \, u_{ji}}{\sum_i a_i \, r_{ij}}$ / sum_r̂ // mean

$\sigma_j^2 = \frac{\sum_i a_i \, r_{ij} \left(u_{ji} - \mu_j\right)^2}{\sum_i a_i \, r_{ij}}$ // variance

cost_j = β_u * sum_r̂ * log (σ_j² + ε) // **cost function**

$a_j = Sigmoid\ \left(\lambda \left(\beta_\alpha - \beta_u . \log \sigma_j^2\right)\right)))$ // **capsule activation**

```
      // E-step: update routing weights based on Gaussian likelihood
      for all capsules i and j:
         p_ij = N (û_ij | μ_j, σ_j²)        // probability under Gaussian
```

$r_{ij} = \frac{a_j . \mathcal{N}\left(u_{ji} | \mu_j, \sigma_j^2\right)}{\sum_k a_k . \ \mathcal{N}\left(u_{ki} | \mu_k, \sigma_k^2\right)}$

```
 normalize r_ij across j for each i
return v_j = μ_j, a_j
```

Pseudocode 2. Pseudocode of EMRCN

3.3. Deep CapsNet

DCN represents a significant advancement in capsule-based architecture by extending the original concept to deeper, more expressive models [27]. While traditional Capsule

Networks offered improved handling of spatial hierarchies and part-whole relationships compared to convolutional neural networks, their relatively shallow structure limited their scalability to more complex real-world tasks. This hierarchical approach mirrors how humans process visual data, from detecting edges and textures to recognizing entire objects or scenes. As a result, DCN achieves superior performance on large-scale and highly variable datasets, where shallow architecture struggles to maintain interpretability and accuracy. The DCN architecture, shown in Figure 3, improves hierarchical learning by adding layers to CapsNet. Initially, a 7x7 convolutional layer (stride 1) collects key spatial characteristics from the input. Each capsule vector receives a Mapping Function after formation. Each capsule vector receives a Mapping Function after formation. This function encodes feature probability by ensuring the output vector length is between 0 and 1. Vector direction denotes posture and part-whole connection, whereas magnitude reflects confidence. In this model, Digit Capsules construct 64-dimensional vectors from these predictions. Each capsule encodes complete information about the expected entity for a class (e.g., digit or object). Each digit capsule vector's length indicates the class's probability. Equation 5 shows the deep iterative routing algorithm, and Equation 6 shows the mapping function.

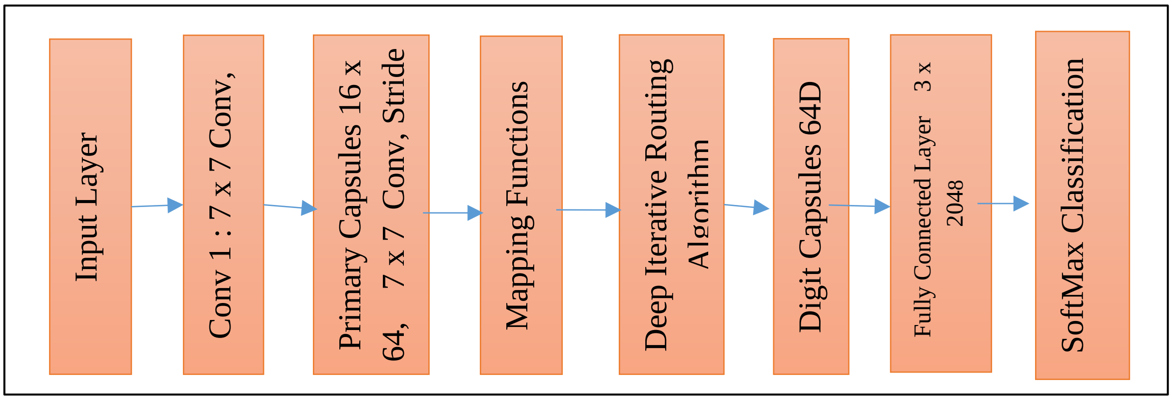

Figure 3. DCN Architecture

$$v_j^{(t+1)} = \text{squash}\left(\sum_i c_{ij}^{(t)} \cdot W_{ij} \cdot u_i^{(t)}\right) \tag{4}$$

$$c_{ij}^{(t)} = \frac{\exp\left(b_{ij}^{(t)}\right)}{\sum_k \exp\left(b_{ij}^{(t)}\right)} \tag{5}$$

where $u_i^{(t)}$ is Output from lower capsule i at iteration t , W_{ij} is Trainable transformation matrix from capsule i to capsule j, $v_j^{(t+1)}$ is Output of higher-level capsule j at iteration $(t+1)$, $c_{ij}^{(t)}$ Coupling coefficient at iteration t , computed by softmax over logits $b_{ij}^{(t)}$. The

Pseudocode (Pseudocode 3) of DCN with 3D convolution-based dynamic routing is as follows.

```
Input:
    x          → Input image
    L          → Number of capsule layers
    r          → Number of routing iterations
Output:
    Class probabilities (Softmax of Digit Capsule lengths)
1. x = NormalizeInput(x)
2. F = Conv2D (filters=256, kernel=5x5, stride=1) (x)      // Initial feature extraction
3. Initialize capsules: C [0] = PrimaryCapsules(F)
4. for l = 1 to L - 1 do:
       for routing iteration t = 1 to r do:
           for each capsule i in layer l and capsule j in layer l+1:
               û_ij = Conv3D (W_ij * C[l][i])          // Prediction using 3D convolution
           c_ij = Softmax (b_ij across j)              // Normalize coupling coefficients
           for each capsule j:
               s_j = ∑_i (c_ij * û_ij)
               v_j = squash(s_j)
           for each i, j:
               b_ij = b_ij + (û_ij · v_j)              // Update logits based on agreement
       C[l+1] = v_j                                    // Update capsule outputs

5. DigitCaps = C[L]                                    // Final capsule layer (class capsules)
6. y_pred = Softmax(||DigitCaps||)                     // Use vector lengths as class scores
return y_pred
```

Pseudocode 3 . Pseudocode of DCN

Table 1 compares the fully connected (FC) layer configurations for DRCN, EMRCN, and DCN. DRCN and EMRCN typically rebuild inputs and classify using two FC layers—one hidden and one output. DCN adds a third FC layer for more complicated feature changes and semantic interpretation. For hierarchical problems, this hidden layer improves model capacity and accuracy. All architectures depend on FC layers to refine capsule outputs into useful classifications and reconstructions.

Table 1. Fully Connected Layers in Capsule Network Architectures

Architecture	**Fully Connected Layers**	**Hidden Layers in FC**	**Functionality of FC Layers**
DRCN	2	1 Hidden, 1 Output	The first layer reconstructs the input from capsule outputs; the second outputs predictions through SoftMax.
EMRCN	2	1 Hidden, 1 Output	Supports reconstruction of the input image and fine-tuned classification output.
DCN	3	2 Hidden, 1 Output	Enables deep semantic reconstruction and improved classification through deeper capsule hierarchies.

4. Results and Discussion

This system of abnormal and normal images was studied from the database of PCOS [28]. The PCOS data set consists of 3856 original images, out of which 1568 are abnormal, 2288 are normal. Figure 4 displays Ultrasound Image Samples of abnormal PCOS in the 1st row and the 2nd row the normal PCOS. Variations in greyscale intensity and resolution emphasize the need for sophisticated image processing methods to improve diagnostic clarity. It depicts normal ovarian morphology, used as baseline standards in PCOS diagnosis methods. The scans do not exhibit the characteristic polycystic characteristics, including numerous peripheral follicles or increased ovarian volume.

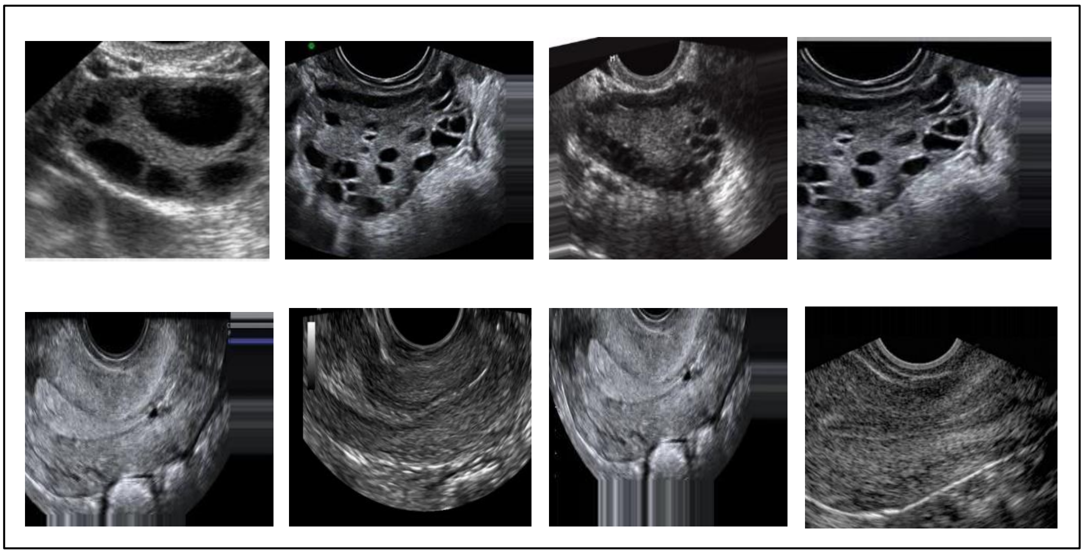

Figure 4. Ultrasound Image Samples – Abnormal and Normal Polycystic Ovary Characteristics

Overfitting occurs when a model performs well on training data but fails to generalize to unseen test data, which is a critical concern in medical imaging due to typically small datasets and subtle but significant visual features. The PCOS database has only 1568 abnormal images and 2288 normal images. To avoid overfitting, data augmentation techniques such as image rotation and flipping are employed, which help the model to learn features across varied image conditions rather than memorizing specific patterns. The proposed system uses 5000 augmented images per class (normal and abnormal) to overcome overfitting due to inadequate actual data. Exposing Capsule Networks to more variations enhances their generalisation. This reduces overfitting and ensures that the model does not depend only on the dataset. Augmentation also enhances feature routing, enabling Capsule Networks to extract and preserve complex patterns more effectively. It improves classification system reliability and performance.

In this study, the dataset is divided into two subsets using a 70:30 split ratio, where 70% of the data is allocated for training and 30% for testing. The training set is used to train the CapsNet model by adjusting its parameters and learning meaningful patterns, while the test set evaluates the model's generalization ability on unseen data. The performance of the system is analyzed using the following performance metrics. Accuracy is a fundamental metric used to evaluate the overall performance of the proposed system. It calculates the ratio of correctly predicted instances (both true positives and true negatives) to the total number of instances. Accuracy is defined as:

$$A = \frac{TP+TN}{TP+TN+FP+FN} \tag{6}$$

Precision is a metric that measures the accuracy of positive predictions by the proposed system for PCOS. It is defined as the ratio of true positives to the sum of true positives and false positives. The formula for Precision is:

$$P = \frac{TP}{TP+FP} \tag{7}$$

Recall, also known as sensitivity or true positive rate, measures the model's ability to identify all actual positive cases. It is defined as the ratio of true positives to the sum of true positives and false negatives, represented by the formula:

$$R = \frac{TP}{TP+FN} \tag{8}$$

The F1 Score is the harmonic mean of precision and recall, providing a balanced measure of both metrics. It is particularly useful when dealing with imbalanced datasets, where one class may dominate the other. The F1 Score is defined as:

$$F1 = 2.\frac{P*R}{P+R} \tag{9}$$

In this approach, the three architectures, namely DRCN, EMRCN, DCN, were studied. The Confusion matrices of all three architectures are shown in Figure 5.

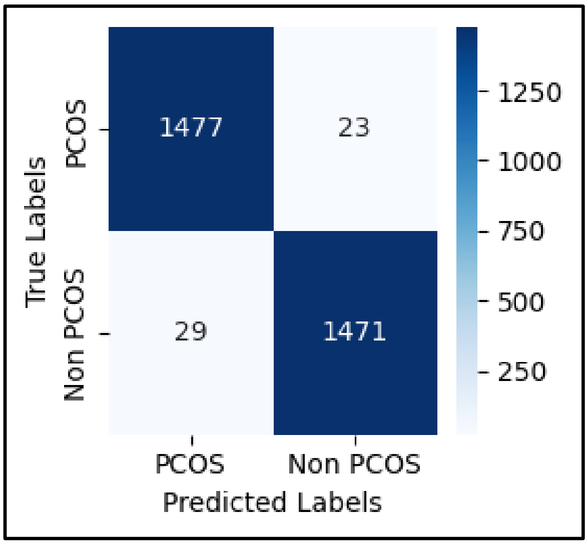

(a)

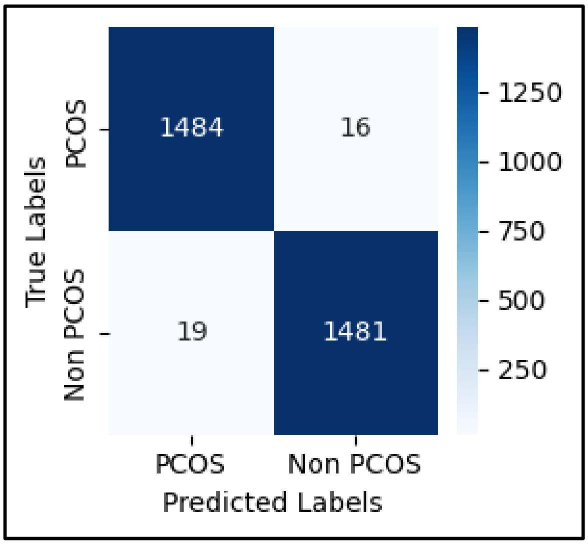

(b)

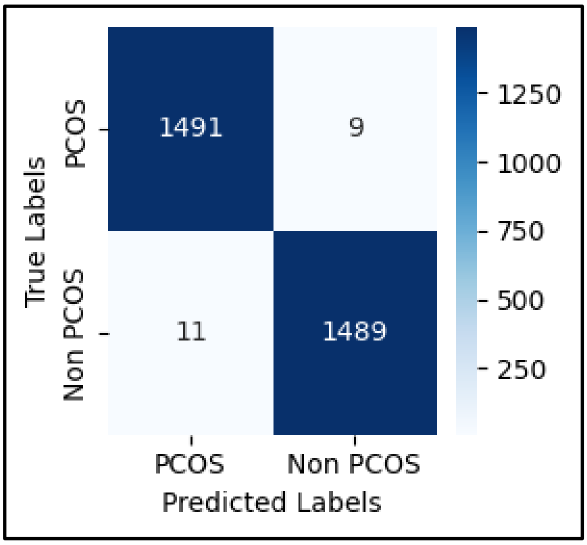

(C)

Figure 5. Confusion Matrics (a) DRCN (b) EMRCN (c) DCN

Table 2 presents the performance metrics of three types of Capsule Networks assessed for the identification of PCOS using medical imaging data using the confusion matrics.

Table 2. Comparative Performance of Routing Variants in Capsule Networks

Model Variant	Accuracy (%)	Precision	Recall	F1 Score
DRCN	98.27	98.07	98.47	98.27
EMRCN	98.83	98.74	98.93	98.83
DCN	99.33	99.27	99.4	99.33

The performance comparison of different Capsule Network routing techniques in Table 2 highlights the superiority of DCN in PCOS classification. With an accuracy of 99.33%, it surpasses EMRCN (98.83%) by 0.50% and DRCN (98.27%) by 1.06%, indicating a more precise classification ability. Additionally, DCN demonstrates a 99.27% precision, reducing false positives more effectively than EMRCN (98.74%) and DRCN (98.07%). Its recall of 99.40% signifies its ability to detect more PCOS cases, outperforming EMRCN (98.93%) and DRCN (98.47%). Its F1-score of 99.33% reflects a well-balanced performance, marking a 0.50% and 1.06% improvement over EMRCN and DRCN, respectively.

The classification error during training is the proportion of incorrect predictions made by a model when trying to assign input data to predefined categories. In ultrasound-based medical image analysis, it measures how often the system incorrectly classifies cases, such as identifying a healthy ovary as polycystic or missing an actual PCOS case. These errors can result from image complexity, anatomical variability, and noise or artifacts commonly present in ultrasound data. Even advanced architectures like capsule networks, which preserve spatial relationships and part-whole hierarchies, can misclassify images, especially in edge cases with subtle or unclear visual indicators. The classification error is mathematically represented by the formula:

$$\text{Classification Error} = \frac{\text{Number of Incorrect Predictions}}{\text{Total Number of Predictions}} \text{ x } 100 \tag{10}$$

A more reliable and accurate model has lower classification error, which is essential in clinical diagnostics where incorrect decisions can significantly impact patient outcomes. Figure 6 and 7 compare the training accuracy and loss of different CapsNet throughout 15 training epochs.

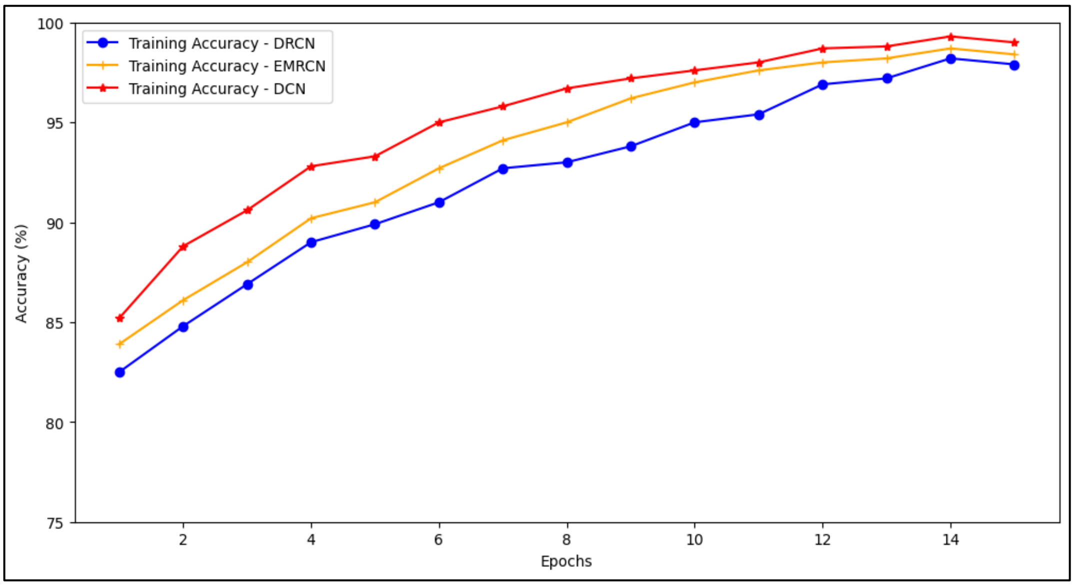

Figure 6. Accuracy vs. Epochs Curve for Three Capsule Network Architectures

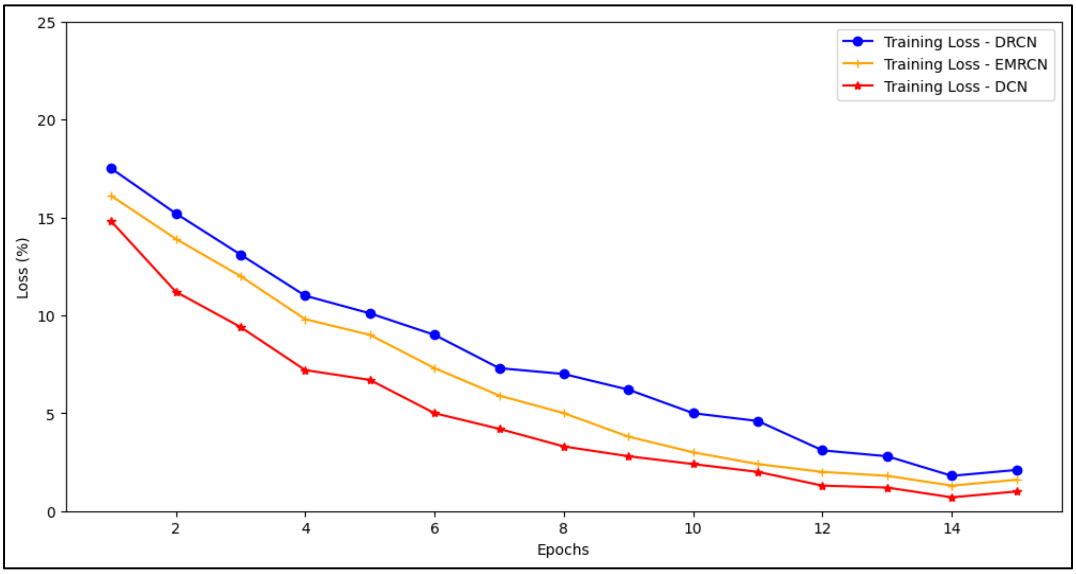

Figure 7. Loss vs. Epochs Curve for Three Capsule Network Architectures

Effective learning and convergence are shown in Figure 6 and Figure 7 by all three models throughout training. To emulate genuine model behaviour like modest overfitting or noise sensitivity, accuracy decreases after epoch 14 and training loss increases. DCN consistently has the best accuracy, followed by EMRCN and DRCN. In complicated medical classification applications, deeper Capsule topologies are more generalisable and stable. Figure 8 shows a bar chart comparing six deep learning architectures for PCOS classification accuracy. CNNs like VGG, AlexNet, and GoogleNet are included, as well as DRCN, EM Routing, and DCN.

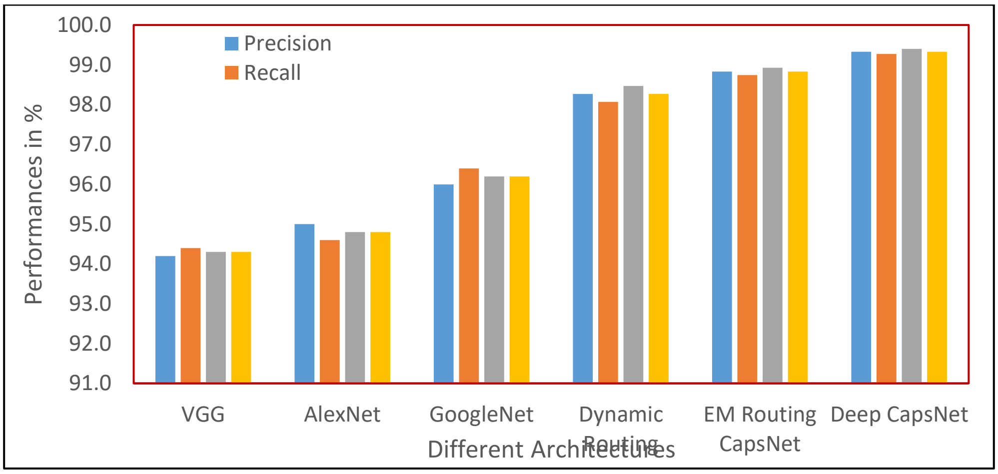

Figure 8. Performance Comparison of CapsNet with State-of-the-Art Deep Learning Architectures

The performance comparison of different architectures, including VGG, AlexNet, GoogleNet, and Capsule Network variants in Figure 8 shows that a clear trend in classification effectiveness. Traditional CNN architectures (VGG, AlexNet, GoogleNet) achieve accuracy ranging from 94.3% to 96.2%, with GoogleNet performing the best among them (96.2% accuracy, 96.4% recall). However, Capsule Networks outperform them significantly.

5. Conclusion

In this research work, different CapsNet are designed for PCOS classification. The design used its routing-by-agreement approach to maintain spatial hierarchies, facilitating accurate interpretation of ovarian morphology, essential for identifying the existence and distribution of follicles linked to PCOS. DCN demonstrated exceptional performance in identifying PCOS with ultrasound imaging data. The classification accuracy of 99.33%, together with a precision of 99.27%, and a recall of 99.4%, emphasized its exceptional diagnostic capability relative to EMRCN and DRCN. The misclassifications by different CapsNet validate its ability to harmonise model complexity with clinical dependability. In contrast to conventional CNNs, which often eliminate pose information through max pooling, capsule-based designs preserve essential spatial signals throughout the learning process. The performances of the proposed systems are analysed with a carfully labelled PCOS ultrasonography dataset including over 3,000 annotated medical images, hence enabling precise benchmarking and model validation.

References

[1] Sumithra, Subramanian, Moorthy Radhika, Gandavadi Venkatesh, Babu Seetha Lakshmi, Balraj Victoria Jancee, Nagarajan Mohankumar, and Subbiah Murugan. "Deep learning for infectious disease surveillance integrating internet of things for rapid response." International Journal of Electrical & Computer Engineering (2088-8708) 15, no. 1 (2025).

[2] PA, Gowri Sankar. "Cervical Cancer Segmentation using Fuzzy Support Vector Machine Algorithm." Journal of Soft Computing Paradigm 6, no. 2 (2024): 201-213.

[3] Allwin, D., Dhaniyasravani, M., & Babu, R. T. S. (2024). CNN-enhanced ECG wearables for cardiac health assessment with arrhythmia prediction. International Journal of Advances in Signal and Image Sciences, 10(1), 13-21.

[4] Jeslin, J. G., Vijayalakshmi, K., Vignesh, C. C., Suresh, G., Kosuri, G. V., & Murugan, S. (2024, October). Predicting Patient Disease Progression with Cloud-based Decision Trees and IoT Data Integration. In 2024 2nd International Conference on Self Sustainable Artificial Intelligence Systems (ICSSAS) IEEE. 1040-1045

[5] Nimmala, Bhargavi, Udaya Deepthi Nimmala, Akhilesh Elangi, and Shilpa Bagade. "PCOS Detection and Monitoring using Machine Learning." In 2024 5th International Conference on Image Processing and Capsule Networks (ICIPCN), IEEE, 2024. 238-242.

[6] Yuan, Yue, Yan Mao, Liu Yang, Yilin Wang, and Xuehong Zhang. "Analysis of macrophage polarization and regulation characteristics in ovarian tissues of polycystic ovary syndrome." Frontiers in Medicine 11 (2024): 1417983.

[7] Zhang, Xudong, Xue Bai, Lina Zhang, Ling Xiong, Juwen Zhang, Yun Li, Wenjing Chang, and Wei Chen. "Kuntai capsule for the treatment of ovulatory disorder infertility: A systematic review and meta-analysis of randomized controlled trials." European Journal of Integrative Medicine 67 (2024): 102350.

[8] Fu, Yu, Manjin Zhang, Bingdong Sui, FeiFei Yuan, Wenbo Zhang, Yashuang Weng, Lei Xiang et al. "Mesenchymal stem cell-derived apoptotic vesicles ameliorate impaired ovarian folliculogenesis in polycystic ovary syndrome and ovarian aging by targeting WNT signaling." Theranostics 14, no. 8 (2024): 3385.

[9] Zhang, Rongrong, Wenjun Xu, Hongquan Wei, Boshi Li, Yaoxing Wang, Xueqing He, Jun Cao et al. "Mechanism of YJKL Decoction in Treating of PCOS Infertility by Integrative Approach of Network Pharmacology and Experimental Verification." Drug Design, Development and Therapy, 2024. 3853-3870.

[10] Lan, Huan, Zhe-Wen Dong, Ming-Yu Zhang, Wan-Ying Li, Chao-Jie Chong, Ya-Qi Wu, Zi-Xian Wang et al. "Sinapic acid modulates oxidative stress and metabolic disturbances to attenuate ovarian fibrosis in letrozole-induced polycystic ovary syndrome SD rats." Food Science & Nutrition 12, no. 4 (2024): 2917-2931.

[11] Hajam, Younis Ahmad, Hilal Ahmad Rather, Rajesh Kumar, Muddasir Basheer, and Mohd Salim Reshi. "A review on critical appraisal and pathogenesis of polycystic ovarian syndrome." Endocrine and Metabolic Science 14 (2024): 100162.

[12] Sajjadi-Jazi, Sayed Mahmoud, Milad Sanginabadi, Behnaz Moradi, Amir Pejman Hashemi Taheri, Mehrnam Amouei, Mostafa Qorbani, Saeed Hosseini et al. "Effect of Oligopin Administration on Ovarian Morphology in Women with Polycystic Ovarian Syndrome (PCOS)." International Journal of Clinical Practice 2024, no. 1 (2024): 6479885.

[13] Setji, Tracy L., and Ann J. Brown. "Polycystic ovary syndrome: diagnosis and treatment." The American journal of medicine 120, no. 2 (2007): 128-132.

[14] Zhang, Jia-Cheng, Hao-Lin Zhang, Xi-Yan Xin, Yu-Tian Zhu, Xin Mao, Hang-Qi Hu, Yu-Xin Jin et al. "Mechanisms of Bushen Tiaoxue Granules against controlled ovarian hyperstimulation-induced abnormal morphology of endometrium based on network pharmacology." Journal of Ovarian Research 17, no. 1 (2024): 25.

[15] Wen, Fan, Yuxi Ding, Mingming Wang, Jing Du, Shen Zhang, and Kehkooi Kee. "FOXL2 and NR5A1 induce human fibroblasts into steroidogenic ovarian granulosa-like cells." Cell Proliferation 57, no. 5 (2024): e13589.

[16] Dutta A., Banerjee R, Banik A, Banerjee Chatterjee M.S., Chakraborty P., Dutta A, and Banerjee A.G., “Polycystic ovarian syndrome: An ongoing public health concern,” Journal of Chemical Health Risks JCHR, vol. 14, no. 1, pp. 2446-2459, 2024.

[17] Wang, Yue, Jie Chen, Han Dong, Rui-Lin Ma, Ying Zou, Wei Wang, Qingmei Zheng et al. "Effect of Consultation Number on the Assessment and Treatment of Polycystic Ovary Syndrome." International Journal of Women's Health (2024): 527-541.

[18] Xu, Yinlong, Xiaoqiang Liu, Zitai Kong, Yixuan Wu, Yue Wang, Yingzhou Lu, Honghao Gao, Jian Wu, and Hongxia Xu. "MambaCapsule: Towards Transparent Cardiac Disease Diagnosis with Electrocardiography Using Mamba Capsule Network." arXiv preprint arXiv:2407.20893 (2024)

[19] Bushara, A. R., RS Vinod Kumar, and S. S. Kumar. "Classification of benign and malignancy in lung cancer using capsule networks with dynamic routing algorithm on computed tomography images." Journal of Artificial Intelligence and Technology 4, no. 1 (2024): 40-48.

[20] Abbassi, Saeid, Kamaledin Ghiasi-Shirazi, and Ahad Harati. "Deep multi-prototype capsule networks." arXiv preprint arXiv:2404.15445 (2024).

[21] Zhai, H. and Zhao, J., 2024. Two-Stream spectral-spatial convolutional capsule network for Hyperspectral image classification. International Journal of Applied Earth Observation and Geoinformation, 127, 103614.

[22] Li, Z., Liu, J., Wang, H., Zhang, X., Wu, Z. and Han, B., 2024. VT-3DCapsNet: Visual tempos 3D-Capsule network for video-based facial expression recognition. Plos one, 19(8), e0307446.

[23] Liu, Han, Changya Li, Xiaotong Zhang, Feng Zhang, Wei Wang, Fenglong Ma, Hongyang Chen, Hong Yu, and Xianchao Zhang. "Depression detection via capsule networks with contrastive learning." In Proceedings of the AAAI Conference on Artificial Intelligence, vol. 38, no. 20, 2024. 22231-22239

[24] Everett, Miles, Aiden Durrant, Mingjun Zhong, and Georgios Leontidis. "Capsule Network Projectors are Equivariant and Invariant Learners." arXiv preprint arXiv:2405.14386 (2024).

[25] Sabour S., Frosst N., and Hinton G.E., “Dynamic routing between capsules,” Advances in neural information processing systems, vol. 30, 1-11, 2017

[26] Hinton, Geoffrey E., Sara Sabour, and Nicholas Frosst. "Matrix capsules with EM routing." In International conference on learning representations. 2018

[27] Rajasegaran, Jathushan, Vinoj Jayasundara, Sandaru Jayasekara, Hirunima Jayasekara, Suranga Seneviratne, and Ranga Rodrigo. "Deepcaps: Going deeper with capsule networks." In Proceedings of the IEEE/CVF conference on computer vision and pattern recognition, 2019. 10725-10733

[28] PCOS dataset: https://www.kaggle.com/datasets/anaghachoudhari/pcos-detection-using-ultrasound-images/data).